Dispersive Phonon Linewidths: The E_2 Phonons of ZnO

J. Serrano,[1,*] F. J. Manjón,[1,2] A. H. Romero,[3] F. Widulle,[1] R. Lauck,[1] and M. Cardona[1]

[1]*Max-Planck-Institut für Festkörperforschung, Heisenbergstrasse 1, 70569 Stuttgart, Germany*

[2]*Departamento de Física Aplicada, Universitat Politècnica de València, E.P.S.A. ES-03801 Alcoy, Spain*

[3]*Advanced Materials Department, IPICyT, 78231 San Luis Potosí, Mexico*

(Received 14 October 2002; published 7 February 2003)

Phonon linewidths can exhibit a large variation when either pressure or isotopic masses are changed. These effects yield detailed information about the mechanisms responsible for linewidths and lifetimes, e.g., anharmonicity or isotopic disorder. We report Raman measurements of the linewidth of the upper E_2 phonons of ZnO crystals with several isotopic compositions and their dependence on pressure. Changes by a factor of 12 are observed at a given temperature. Comparison with calculated densities of one-phonon states, responsible for isotope scattering, and of two-phonon states, responsible for anharmonic decay, yields a consistent picture of these phenomena. Isotopic disorder broadening by 7 cm^{-1} is found in samples with mixed ^{16}O–^{18}O content, whereas the anharmonic processes involve decay into sums and differences of two phonons.

DOI: 10.1103/PhysRevLett.90.055510 PACS numbers: 63.20.Kr, 63.20.Dj, 78.30.Fs

Considerable progress has been made in recent years in the understanding of the mechanisms which determine phonon linewidths [1–3]. The relevant experimental database has been obtained mainly by Raman spectroscopy on samples with diverse isotopic compositions and under hydrostatic stress [4]. The theoretical underpinnings have been extracted from *ab initio* electronic structure calculations, mostly for diamond- and zinc-blende-type semiconductors [5]. Unfortunately, these materials have only one set of Raman-active phonons because of the presence of only two atoms per primitive cell (PC).

In this Letter we investigate the technologically important material ZnO whose wurtzite structure allows four sets of Raman-active phonons of symmetries A_1, E_1, and $2E_2$. We concentrate on the upper E_2 phonon, E_2^{high}, located at 439 cm^{-1} at 300 K for the natural isotopic abundances, and show that its width can change by as much as a factor of 5 upon application of pressure and 12 by changing the isotopic composition.

Natural ZnO has a mixed isotopic zinc composition but nearly isotopically pure ^{16}O. This results in negligible isotopic disorder effects for the E_2^{high} modes since they involve mainly oxygen displacements. In samples with $^{16}O_{0.5}{}^{18}O_{0.5}$ composition, a large broadening of the E_2^{high} mode is observed and analyzed on the basis of standard perturbation theory using an *ab initio* calculated one-phonon density of states (DOS). For samples containing only natural oxygen or pure ^{18}O the phonon linewidth is determined by anharmonic decay into pairs of phonons. Accidentally, the phonon frequency lies on a steep and structured ridge of the two-phonon (sum) DOS. The anharmonic width can thus be varied widely by application of pressure, which displaces the E_2^{high} frequency along the ridge, and also by isotopic mass substitution, since the E_2^{high} frequency depends almost only on the oxygen mass, whereas the two-phonon DOS depends only on the zinc mass in that region. Measurements of these effects at 7 K and at 300 K yield a consistent picture of the mechanisms which determine the linewidth of the E_2^{high} phonons: anharmonic decay into sums and differences of phonons plus elastic scattering in the crystals with mixed isotopic oxygen composition.

We have performed Raman measurements on ZnO grown by chemical vapor transport with NH_4Cl as transporting agent and a source temperature of 900 °C [6]. As starting constituents we have used ^{64}Zn, ^{68}Zn, ^{18}O, and natural oxygen (99.76% ^{16}O), the first three elements having an isotope purity of $\approx 99\%$. Crystals with all four combinations of the "pure" isotopes, as well as natural zinc, with an average mass of 65.39 amu, were grown. We also grew crystals with $^{64}Zn_{0.5}{}^{68}Zn_{0.5}$ and $^{16}O_{0.5}{}^{18}O_{0.5}$ so as to investigate isotopic disorder effects.

The Raman measurements were performed using the 676, 568, and 514 nm lines from a Kr^+-Ar^+ mixed gas laser, the resolution obtained being, of course, higher with the 676 nm line, i.e., 0.6 cm^{-1} for measurements at low temperature and 2 cm^{-1} at high temperature. The pressure was applied at room temperature with a diamond anvil cell, with a 4:1 methanol-ethanol mixture as pressure transmitting fluid. Such a mixture gives hydrostatic pressures within the resolution at hand and the pressure range under consideration, 0–8 GPa [7]. The measurements, involving different pressures, temperatures, and isotopic composition, were restricted to the E_2^{high} Raman-active phonons of ZnO for which we were aware that anomalies took place [8–10]. Cursory checks for the other Raman phonons did not show any effects as striking as the ones discussed here. The E_2^{low} phonon was found to be extremely narrow, well below our spectral resolution especially at low temperature (≤ 0.1 cm^{-1}) [11].

Figure 1 shows three typical Raman spectra at 7 K, two obtained for $^{64}Zn^{18}O$ and $^{68}Zn^{16}O$ with a spectral

 0031-9007/03/90(5)/055510(4)$20.00

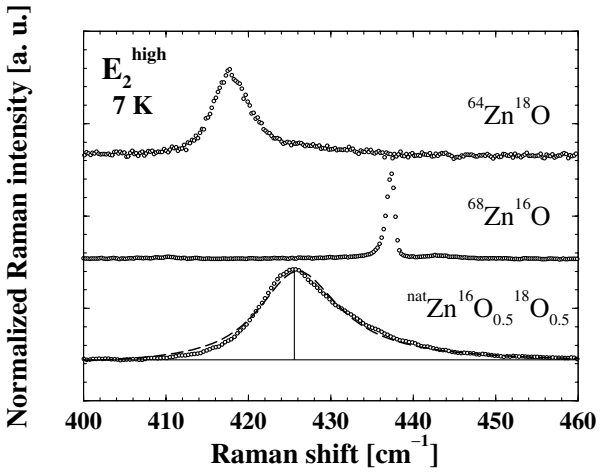

FIG. 1. Raman spectra of the E_2^{high} phonons at 7 K for three ZnO samples. Note the broad and asymmetric spectrum of the $^{16}O_{0.5}{}^{18}O_{0.5}$ sample. The dashed line is a fit with a Lorentzian including spectral resolution, the anharmonic contribution and the disorder effects (see text).

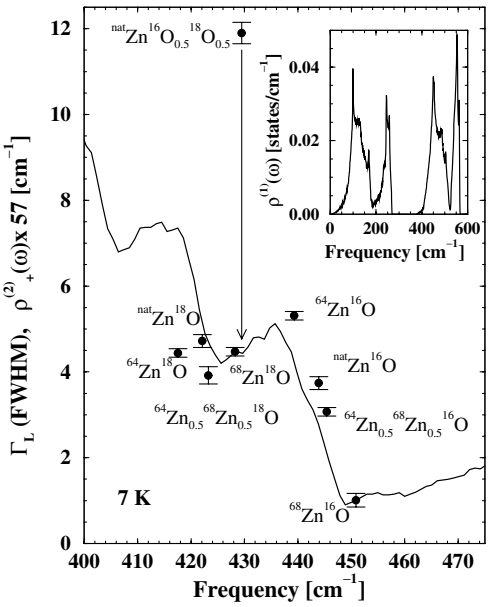

FIG. 2. Resolution-corrected FWHM of the E_2^{high} phonons obtained from 7 K Raman spectra for several isotopic compositions. The points corresponding to $^{64}Zn^{x}O$ samples are plotted at the measured frequencies, the others have been shifted as explained in the text. The solid line displays the calculated $\rho^{(2)}_+(\omega)$ scaled by a factor of 57 cm^{-2}. The large width observed for $^{nat}Zn^{16}O_{0.5}{}^{18}O_{0.5}$ illustrates the effect of isotopic mass fluctuations. Similar values of FWHM were found for other samples containing the same mixture of O isotopes. The inset displays the one-phonon DOS, $\rho^{(1)}(\omega)$.

resolution of full width at half maximum (FWHM) equal to 0.6 cm^{-1}. The deconvoluted Lorentzian FWHM, Γ_L, can be easily obtained from those in Fig. 1 using [12]

$$\Gamma_L = \Gamma - \frac{\Gamma_G^2}{\Gamma}, \tag{1}$$

where Γ is the measured FWHM and Γ_G that of the lines obtained from a calibration neon lamp which yields Gaussian line shapes. This procedure leads to $\Gamma_L \approx 4.5$ cm^{-1} for $^{64}Zn^{18}O$ and $\Gamma_L \approx 1$ cm^{-1} for $^{68}Zn^{16}O$, a rather remarkable change. The Raman spectrum of $^{nat}Zn^{16}O_{0.5}{}^{18}O_{0.5}$ of Fig. 1, ^{nat}Zn representing the natural element, was measured with a resolution of 2 cm^{-1}. Its large and asymmetric width reveals the effect of the mass fluctuations of the oxygen atoms, that of the zinc fluctuations being nearly negligible since the E_2^{high} mode corresponds ($\approx 85\%$ [8,13]) to a vibration of the oxygen atoms. We have observed an effect of the zinc mass fluctuations on the E_2^{low} phonon, but it is not discussed here in detail. The dashed line through the experimental points for the isotopically mixed sample of Fig. 1 represents a theoretical fit to be discussed below.

Figure 2 displays the frequency dependence of the widths of the E_2^{high} phonons of all isotopically pure crystals and those containing natural and $^{64}Zn_{0.5}{}^{68}Zn_{0.5}$ mixed zinc compositions measured at low temperature. The effect of the spectral resolution has been removed with Eq. (1). The line through the points represents the DOS for sums of two phonons with equal $\mathbf{q}$ vectors calculated from the *ab initio* lattice dynamics [8,13]. Raman phonons, at $\mathbf{q} \simeq 0$, are known to decay mainly into such combinations [1–5]. The frequency range of Fig. 2 corresponds to a sum of transverse and longitudinal acoustic phonons (TA + LA) in the vicinity of the *K* point of the Brillouin zone. The frequency of these phonons varies like $M_{Zn}^{-1/2}$, where M_{Zn} is the average mass of the zinc atoms, and is nearly independent of the oxygen mass, a conjecture that was checked by changing the isotopic masses in the *ab initio* calculation. The experimental points of the ^{64}Zn samples were plotted at the measured frequencies, whereas those with other zinc masses were shifted to take into account the $M_{Zn}^{-1/2}$ dependence of the abscissa of the two-phonon DOS, $\rho^{(2)}_+(\omega)$. We note in Fig. 2 that the experimental points follow rather well the calculated dependence of $\rho^{(2)}_+(\omega)$ on frequency. The factor of 57 cm^{-2}, by which $\rho^{(2)}_+(\omega)$ had to be multiplied to reproduce the measured FWHM, represents the corresponding average anharmonic squared matrix element which was found to have the rather similar values of 56 cm^{-2} for GaP [14] and 70 cm^{-2} for CuCl [15]. This matrix element thus seems to increase with increasing ionic character of the material. Notice that the calculated curve reproduces the experimental trend and also reveals the large difference in widths between $^{64}Zn^{18}O$ and $^{68}Zn^{16}O$ already mentioned in connection with Fig. 1.

Figure 3 displays the pressure dependence of the FWHM of the E_2^{high} phonon peaks of $^{nat}Zn^{16}O$, $^{64}Zn^{16}O$, and $^{64}Zn^{18}O$ measured at room temperature for pressures up to 8 GPa. At this pressure a transition to the rocksalt

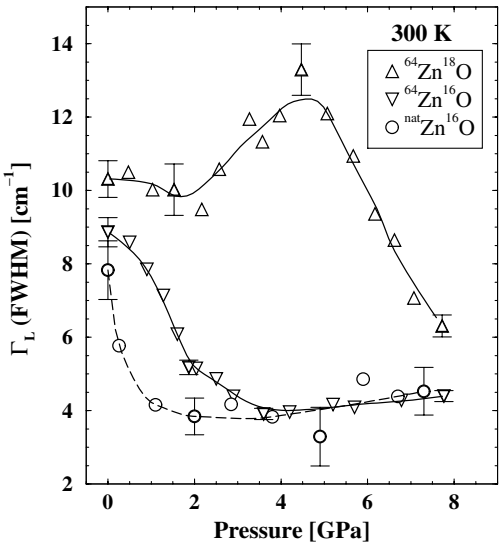

FIG. 3. Effect of hydrostatic pressure on the linewidths of three ZnO samples after correcting for spectral resolution. The measurements were performed at 300 K. The lines are guides to the eye.

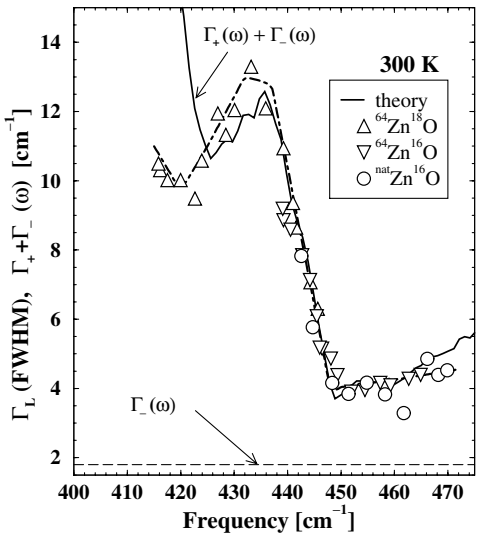

FIG. 4. Experimental points of Fig. 3 replotted vs peak frequency, with the frequency shifts and scaling described in the text. The solid line was obtained by adding to the $\Gamma_+(\omega)$ of Eq. (2) a constant attributed to $\Gamma_-(\omega)$ (dashed line).

phase occurs [9,10]. The widths in Fig. 3 have been corrected for spectral resolution with Eq. (1) using $\Gamma_G = 2\ \mathrm{cm}^{-1}$. The maximum width shown in Fig. 3, for $^{64}Zn^{18}O$, is 13 cm^{-1}, whereas a minimum width of 3.5 cm^{-1} is seen for the $^{nat}Zn^{16}O$ sample. The nonmonotonic changes with pressure seen in Fig. 3 correspond rather well to the features in $\rho_+^{(2)}(\omega)$ displayed in Fig. 2. The difference between the curves in Fig. 3, drawn as a guide to the eye through the measured points, arises from the different zero pressure frequencies for the three samples.

In order to compare these curves with $\rho_+^{(2)}(\omega)$, one has first to rescale the frequencies with the zinc mass using one, i.e., ^{64}Zn, as reference, as done for Fig. 2. Then, we must take into account the shift of $\rho_+^{(2)}(\omega)$ with pressure and subtract it from the mass-renormalized frequencies. The pressure dependence of $\rho_+^{(2)}(\omega)$ was obtained from *ab initio* calculations performed at 0, 4, and 8 GPa [13]. After this process, the experimental points of Fig. 3 coalesce into a single curve, as displayed in Fig. 4. The agreement among the three sets of measurements and the calculated DOS is excellent provided one adds a constant background to $\rho_+^{(2)}(\omega)$. Subtraction of this background makes the ratio of maximum to minimum width of about five seen in Fig. 2 equal to that in Fig. 4, as expected for a mechanism involving decay into the sum of two phonons of frequencies ω_1 and ω_2, which leads to the temperature dependent width

$$\Gamma_+(\omega) = B_+\rho_+^{(2)}(\omega)[1 + n_{\mathrm{BE}}(\omega_1) + n_{\mathrm{BE}}(\omega_2)], \qquad (2)$$

where $\omega = \omega_1 + \omega_2$, $n_{\mathrm{BE}}(\omega)$ are Bose-Einstein factors, and $B_+ = 57\ \mathrm{cm}^{-2}$ is the anharmonic squared matrix element. The calculated dispersion relations of ZnO yield $\omega_1 \approx 250\ \mathrm{cm}^{-1}$ and $\omega_2 \approx 190\ \mathrm{cm}^{-1}$. According to Eq. (2) the ratio of the widths for either two different samples or pressures should be independent of temperature.

We now explain the background of $\approx 2\ \mathrm{cm}^{-1}$ used in Fig. 4, but not in Fig. 2, as a decay into differences of two phonons represented by $\rho_-^{(2)}(\omega)$. This contribution is

$$\Gamma_-(\omega) = B_-\rho_-^{(2)}(\omega)[n_{\mathrm{BE}}(\omega_2) - n_{\mathrm{BE}}(\omega_1)], \qquad (3)$$

where $\omega = \omega_1 - \omega_2$, and $\omega_{1,2}$ are the average frequencies which contribute to the difference mode. B_- is an adjustable parameter corresponding to the anharmonic squared matrix element. $\rho_-^{(2)}(\omega)$ extends from $\omega = 0$ to ω_{Max}, where ω_{Max} is the highest phonon frequency $\approx 550\ \mathrm{cm}^{-1}$ [8,13]. A calculation [13] reveals that $\rho_-^{(2)}(\omega)$ is almost flat in the 400–460 cm^{-1} region of interest in Figs. 2 and 4, $\rho_-^{(2)}(\omega) \approx 0.25$ states/cm^{-1} per PC. It also shows that ω_1 is a longitudinal optic mode of average frequency $\approx 550\ \mathrm{cm}^{-1}$, whereas $\omega_2 \approx 110\ \mathrm{cm}^{-1}$ has TA character. According to Eq. (3), $\Gamma_-(\omega)$ can be neglected at 7 K, whereas $n_{\mathrm{BE}}(\omega_2) - n_{\mathrm{BE}}(\omega_1) \approx 1.36$ at 300 K. The dashed line of Fig. 4 can therefore be assigned to $\rho_-^{(2)}(\omega)$ and the corresponding matrix element squared is $B_- = 6.3\ \mathrm{cm}^{-2}$, considerably smaller than that which corresponds to $\rho_+^{(2)}(\omega)$, $B_+ = 57\ \mathrm{cm}^{-2}$.

For completeness, we display in Fig. 5 all data collected at 300 K for crystals containing either ^{16}O or ^{18}O with the frequencies shifted as done in Fig. 2 in order to compare them with a single $\rho_+^{(2)}(\omega)$ curve. For the sake of clarity the pressure data of Fig. 4 have been replaced by a

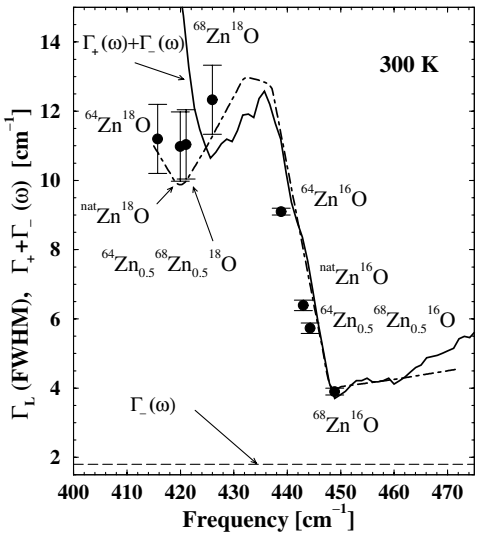

FIG. 5. Linewidths of ZnO with several isotopic compositions at 300 K, after correction for resolution. The solid line represents $\Gamma_+(\omega) + \Gamma_-(\omega)$, from Eqs. (2) and (3). The points have been shifted as done in Fig. 2. The dot-dashed line indicates the pressure dependence shown in Fig. 4.

smooth dot-dashed curve drawn through the experimental points. All isotopes measured at zero pressure agree with this curve within error bars.

Finally, we discuss the effect of the oxygen mass fluctuations on the E_2^{high} linewidths as determined at 7 K and at 300 K for samples containing $^{16}O_{0.5}{}^{18}O_{0.5}$. Four different samples were measured containing ^{64}Zn, ^{68}Zn, ^{nat}Zn, and $^{64}Zn_{0.5}{}^{68}Zn_{0.5}$, respectively. The 7 K Raman spectrum for $^{nat}Zn^{16}O_{0.5}{}^{18}O_{0.5}$, as displayed in Fig. 1, shows a FWHM equal to 12 cm^{-1}, 7 cm^{-1} larger than the expected value of 5 cm^{-1} which can be read off Fig. 2 (see arrow). A similar increase in FWHM is found to be induced by the isotopic disorder at 300 K, as expected.

The isotopic disorder effect for the FWHM of the E_2^{high} phonons of ZnO can be calculated with [3]

$$\Gamma_{iso} = g_2 \frac{\pi}{6} \omega^2 \rho^{(1)}(\omega) |e_O|^4, \qquad (4)$$

where g_2 is the oxygen mass variance ($g_2 = 3.5 \times 10^{-3}$ for $^{16}O_{0.5}{}^{18}O_{0.5}$), $\rho^{(1)}(\omega)$ is the one-phonon DOS, and e_O is the eigenvector component of the oxygen for the mode under consideration. $\rho^{(1)}(\omega)$, as calculated for the *ab initio* lattice dynamics, has a sharp peak with a maximum slightly above the E_2^{high} frequency (see the inset in Fig. 2). At this frequency, $\rho^{(1)}(\omega) \approx 0.021$ states/cm^{-1} per PC and $|e_O|^2 \approx 0.85$ [8]. Using Eq. (4) we thus find $\Gamma_{iso} \approx 5.05$ cm^{-1}, in reasonable agreement with the value determined above. It is also possible to calculate "*ab initio*" the asymmetric profile of E_2^{high} given in Fig. 1 for $^{nat}Zn^{16}O_{0.5}{}^{18}O_{0.5}$. For this purpose we approximate the calculated $\rho^{(1)}(\omega)$ by a quadratic polynomial fit and replace the corresponding Γ_{iso} of Fig. 4 into a Lorentzian expression. We obtain in this manner the dashed line through the experimental points given in Fig. 1.

In summary, we have performed Raman measurements of the E_2^{high} phonons of ZnO with several isotopic compositions at 7 K and at 300 K, and pressure dependence measurements at 300 K. Striking differences are found in the linewidth at low and high temperatures between the different samples, together with a nonmonotonic dependence of the linewidth on pressure. This unusual behavior can be explained by the existence of a steep ridge in the two-phonon DOS and its mass and pressure dependence, obtained with the aid of first principles calculations. The role played in the linewidth by isotopic oxygen mass fluctuations is also reproduced by the enhanced one-phonon DOS using perturbation theory. This DOS is responsible for the asymmetric line shape observed in the spectra of samples containing mixed oxygen isotopes.

We are indebted to I. Loa for a critical reading of the manuscript. We have benefited from discussions with A. Rubio and A. Polian, and we thank K. Syassen for allowing us to use his pressure equipment. F. J. M. and A. H. R. acknowledge support by the *"Programa Incentivo a la investigación de la U.P.V."* and by Millennium Conacyt, Initiative Mexico, Grant No. W-8001, respectively. M. C. also thanks the Fonds der Chemischen Industrie for support.

*Corresponding author.
Electronic address: J.Serrano@fkf.mpg.de

[1] M. Canonico *et al.*, Phys. Rev. Lett. **88**, 215502 (2002).
[2] M. Cardona and T. Ruf, Solid State Commun. **117**, 201 (2001).
[3] F. Widulle, J. Serrano, and M. Cardona, Phys. Rev. B **65**, 075206 (2002).
[4] C. Ulrich *et al.*, Phys. Rev. Lett. **78**, 1283 (1997); F. J. Manjón *et al.*, Phys. Rev. B **64**, 064301 (2001).
[5] A. Debernardi, S. Baroni, and E. Molinari, Phys. Rev. Lett. **75**, 1819 (1995).
[6] R. Lauck (unpublished).
[7] G. J. Piermarini, S. Block, and J. D. Barnett, J. Appl. Phys. **44**, 5377 (1973).
[8] J. Serrano *et al.*, Phys. Status Solidi (b) **235**, 260 (2003).
[9] F. Decremps *et al.*, Phys. Rev. B **65**, 092101 (2002). A change in the width of E_2^{high} with pressure can be seen in Fig. 1 of this work.
[10] F. J. Manjón, K. Syassen, and R. Lauck, High Press. Res. **22**, 299 (2002).
[11] B. H. Bairamov *et al.*, Phys. Status Solidi (b) **119**, 227 (1983).
[12] J. F. Kielkopf, J. Opt. Soc. Am. **63**, 987 (1973).
[13] A. H. Romero (unpublished). The calculated pressure dependence for the ridge is ≈ 1.56 cm^{-1}/GPa.
[14] F. Widulle *et al.*, Phys. Rev. Lett. **82**, 5281 (1999).
[15] A. Göbel *et al.*, Phys. Rev. B **56**, 210 (1997).